Amino Acid Discrimination by a Highly Differentiated Metal Center of an Aminoacyl-tRNA Synthetase[†]

Chun-Mei Zhang,[‡] John J. Perona,[§] and Ya-Ming Hou*,[‡]

Department of Biochemistry and Molecular Pharmacology, Thomas Jefferson University, Philadelphia, Pennsylvania 19107, and Department of Chemistry and Biochemistry, University of California, Santa Barbara, California 93106-9510

ABSTRACT: *Escherichia coli* cysteinyl-tRNA synthetase (CysRS) achieves high amino acid specificity without the need for an editing reaction. Crystallographic and spectroscopic studies have previously demonstrated that a major determinant of the specificity is an active site zinc ion that recognizes the substrate cysteine through a strong zinc−thiolate interaction. The active site cleft of CysRS is composed of highly or strictly conserved amino acids, including four inner-sphere zinc ligands, five histidine imidazoles at the base of the cleft, and a tryptophan that flips down upon cysteine binding to complete formation of the binding pocket. Here we establish the significance of each of these major features of the active site cleft by mutational analysis. Substitutions generally lead to substantially deleterious effects on K_m and k_{cat} parameters with respect to each of the cysteine, ATP, and tRNA^Cys substrates. These findings emphasize the importance of the highly differentiated nature of the active site and provide new insights into the origins of selectivity without editing. Most mutants are less attenuated in tRNA aminoacylation than in adenylate synthesis, suggesting that tRNA binding drives a conformational change to help assemble the active site.

Aminoacyl-tRNA synthetases (AARSs) establish the genetic code by matching amino acids with trinucleotide sequences encoded as the anticodons in tRNAs. Each of the 20 synthetases catalyzes a two-step aminoacylation reaction, whereby an amino acid is first condensed with ATP to form an activated aminoacyl adenylate intermediate, which is then transferred to the 2′- or 3′-terminal hydroxyl group of the cognate tRNA by trans esterification (*1*). Structural studies show that the 20 synthetases can be divided into two classes possessing distinct active site domain architectures (*2*, *3*). In class I synthetases, the active site is composed of the Rossmann fold domain, and the conserved HIGH and KMSKS motifs help to form the ATP-binding site. By contrast, class II synthetases possess an unrelated mixed $\alpha\beta$ active site domain. Adjacent to the class-specific ATP-binding motifs is a pocket that binds the cognate amino acid substrate. Due to the chemical and structural similarities of some amino acids, a number of synthetases from both class I and class II can bind and activate closely similar amino acids in the amino acid pocket. The misaminoacylated tRNA is then hydrolyzed in a spatially separate editing site (*4*– *11*). The editing reaction is energy-consuming and requires hydrolysis of additional ATP (*12*).

Escherichia coli CysRS[1] is a class I synthetase that achieves amino acid specificity without the need for an editing reaction (*13*). Recent crystal structure analysis and spectroscopic studies of the enzyme have demonstrated that the specificity depends on an active site zinc ion that forms a zinc−thiolate bond with the substrate cysteine (*14*, *15*). The crystal structures of the apo- and cysteine-bound forms of the enzyme show a zinc ion located at the very base of the active site cleft (*14*). In the apo form, the zinc ion is coordinated to the side chains of C28, C209, H234, and E238 in an inner-sphere structure that is intermediate between tetrahedral and trigonal bipyramidal states (Figure 1A). All four side chains are strictly conserved, except in two archaeal enzymes where C209 is replaced by an aspartate. Upon binding of the substrate cysteine, the zinc ion moves toward the thiol of cysteine by 0.8 Å, while lengthening the inner-sphere distance to E238 from 2.3 to 3.1 Å. In the new position, the zinc ion is coordinated by the substrate cysteine thiol and by the side chains of the original ligands in a nearly perfect trigonal- bipyramidal geometry (Figure 1B). The direct metal−thiolate interaction has been confirmed by spectroscopic analysis of Co^{2+}-substituted *E. coli* CysRS (*15*). Co^{2+} is similar to Zn^{2+} in chemical and geometric properties but is distinguished by a well-established absorption spectrum in the UV−visible range (*16*). The Co^{2+}-substituted CysRS retains the full activity of the native Zn^{2+} enzyme and displays spectral changes characteristic of formation of a metal−thiolate bond upon cysteine binding. These changes are not observed in the presence of noncognate amino acids and are sensitive to mutations in the metal center (*15*).

Crystal structures of *E. coli* CysRS at 2.3 Å resolution reveal a well-differentiated and highly conserved zinc center which extends beyond the immediate ligation sphere (*14*). Five strictly conserved histidines (H206, H224, H234, H235,

---

* Corresponding author. Phone: 215-503-4480. Fax: 215-923-9162. E-mail: Ya-Ming.Hou@mail.tju.edu.
[‡] Thomas Jefferson University.
[§] University of California, Santa Barbara.
[1] Abbreviations: CysRS, cysteinyl-tRNA synthetase; XNY, mutant CysRS with amino acid X at position *N* replaced by *Y*.
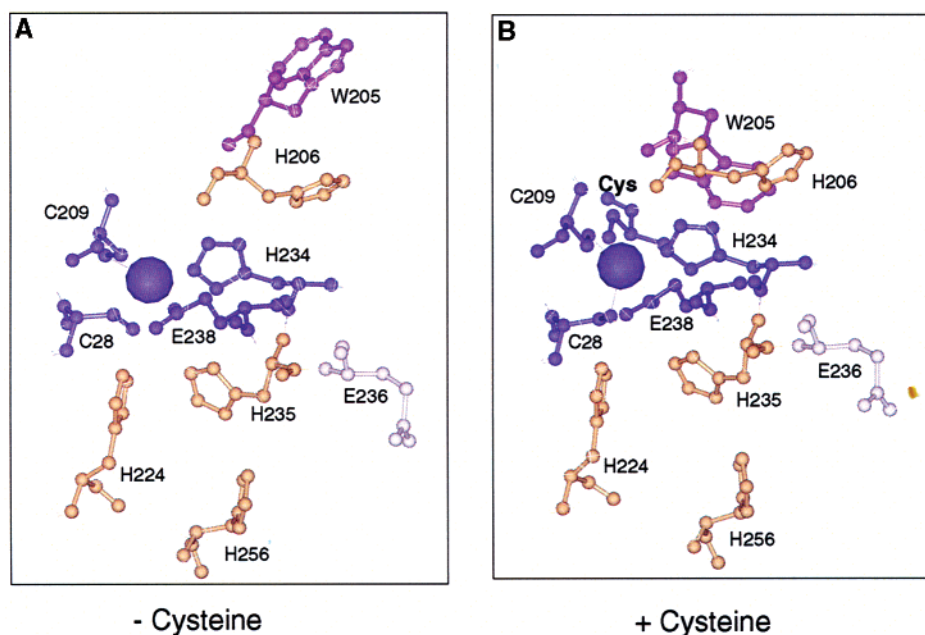
FIGURE 1: Structures of the zinc center in the (A) apo-bound and (B) cysteine-bound *E. coli* CysRS, displaying the zinc ion as a solid ball, direct ligands in blue, the histidine array in brown, and W205 in purple.

and H256) are present at the base of the active site, of which only H234 directly ligates zinc. The imidazole rings of H206, H234, H235, and H256 are roughly in-line and are separated by 4.1 Å or less from each other in the two available structures. The remaining histidine, H224, is positioned between C28 and E238 above the plane of the others. To our knowledge this arrangement of histidines is unique among known protein structures, and the strict conservation suggests an important functional role. In addition, the strictly conserved W205 side chain, which faces the insertion domain in the unligated enzyme, flips down toward the active site upon cysteine binding to stack on the cysteine thiol. This rearrangement appears to be a necessary step to complete formation of the amino acid binding cleft.

While the zinc in CysRS is the major determinant for selectivity of cysteine, the role of the conserved amino acids in the zinc center has not been directly tested. The primary question of interest is whether these amino acids contribute to catalysis of aminoacylation or to structural organization of the enzyme through their ability to bind the zinc. To address this question, each of the conserved side chains has been examined by mutational analysis. Interestingly, substitutions of the majority of the side chains have a deleterious effect on catalysis, without perturbing the global folding of CysRS. We also find that the deleterious effect on catalysis is generally stronger on cysteine than on ATP in adenylate synthesis, consistent with the proximity of these side chains to the cysteine-binding site. Unexpectedly, the catalytic defect is less severe in tRNA aminoacylation than in adenylate synthesis, suggesting a role for tRNA in helping to assemble a proficient active site. Further, individual replacements of direct zinc ligands generally do not significantly compromise zinc binding, suggesting the possibility of an unusual mechanism that sequesters the zinc. Together with the demonstrated difficulty in isolating misactivating mutants, these results reveal an extremely well differentiated amino acid binding cleft that places the zinc ion in the optimal position for substrate selection without editing.

MATERIALS AND METHODS

Enzyme Overexpression, Purification, and Assays. The wild-type *E. coli* CysRS containing a C-terminal His tag was expressed and purified from *E. coli* BL21(DE3) harboring the plasmid pCysRS09, which is a derivative of pET-22b (+). Mutations in CysRS were generated by QuikChange site-directed mutagenesis (Stratagene) from pCysRS09 and were confirmed by sequence analysis. All His-tagged enzymes were purified by the Talon metal-affinity resin (ClonTech) followed by the monoQ column on an FPLC. Enzyme concentrations were determined by the active site burst assay (*17*), based on protein concentrations determined by the Bradford method (Bio-Rad). Assays for amino acid activation by the PP_i−ATP exchange method (*18*) and for aminoacylation of the T7 transcript of *E. coli* tRNA^{Cys} (*19*) were as described. Kinetic parameters K_m, k_{cat}, and k_{cat}/K_m were derived from the Lineweaver−Burk analysis, where the active enzyme concentrations were at least 10-fold below the lowest concentrations of the substrate. Data were fitted to the Michaelis−Menten equation and reported as the average of at least three independent measurements. For enzymes possessing extremely weak activities, only the k_{cat}/K_m value could be obtained. This parameter was determined by measuring the initial rate of reaction at substrate concentrations where no saturation was detected.

Metal Analysis. Zinc analysis was by atomic absorption spectroscopy at the MSI Analytical Laboratory, University of California, Santa Barbara. The samples were diluted to a final concentration of 1 μg/mL in 20 mM Tris-HCl, pH 7.5, and 0.2 mM DTT prior to the analysis, and replicate readings were taken to obtain an average. The human carbonic anhydrase, which contains 1 mol of Zn/mol of enzyme, yielded a value of 0.98 ± 0.01 mol of zinc/mol of enzyme. The standard was prepared from zinc oxide (Fisher certified atomic absorption standard, P/N SO-Z-13, 1000 ppm) dissolved in diluted nitric acid.

Circular Dichroism Analysis of Enzymes. Wild type and variants of *E. coli* CysRS (0.5 μM) were prepared in a buffer containing 20 mM Tris-HCl, pH 7.5, and 1 mM DTT. The spectra were collected on a JASCO J-810 spectrophotometer, and the data were collected at 200−260 nm at room temperature.

Binding of tRNA^{Cys} by Fluorescence Titration. Wild type and variants of *E. coli* CysRS were titrated with increasing concentrations of the T7 transcript of *E. coli* tRNA^{Cys}. The binding reaction was performed in 25 mM sodium acetate, pH 6.0, 10 mM MgCl$_2$, and 5 mM DTT for 10 min at 30 °C and analyzed on a PTI fluorometer (814 Photomultiplier Detection System), using the software Felix (for Windows) version 1.42b. Data were collected with an excitation wavelength of 285 nm, and emission was monitored at 310−400 nm. Addition of tRNA^{Cys} quenches the fluorescence emission. The titration was with 0.625 μM enzyme and was monitored at the wavelength of 330 nm, and the equilibrium dissociation constant for tRNA^{Cys} was obtained by fitting the data with Sigma Plot.

RESULTS

Design of Mutations. The majority of the conserved residues in the zinc center were mutated to serine, which binds Zn^{2+} weakly and which may be less perturbing to the structure than the alanine substitution. All of the mutants were expressed in *E. coli* as C-terminal His-tag fusions, facilitating purification of the mutants away from the chromosome encoded wild-type enzyme. The His-tag addition does not hinder the activity of *E. coli* CysRS in either adenylate synthesis or tRNA aminoacylation. In both reactions, steady-state kinetic parameters of the wild-type enzyme with and without the tag are indistinguishable (*15*).

The activities of the mutants were evaluated for both adenylate synthesis and tRNA aminoacylation. To ensure steady-state conditions, enzyme concentrations were maintained at least 10-fold below those of the substrate. While achieving saturating levels of cysteine for measurement of the K_m for ATP in adenylate synthesis presented no difficulty, that of the K_m for cysteine was performed under subsaturating concentrations of ATP (5 mM) due to the insolubility of ATP in the PP$_i$−ATP exchange assay. This limitation prevents accurate estimation of cysteine parameters for mutants possessing significantly weakened ATP affinities. As such, evaluation in these cases was made only by the measurement of k_{cat}/K_m. The necessity for low ATP concentrations rationalizes why values of k_{cat} determined in some cysteine titrations are lower than corresponding values for ATP titrations (Tables 1 and 2). Similar considerations apply to the tRNA aminoacylation reaction, because of limitations in the concentration of commercially available [^{35}S]cysteine.

Mutations of Direct Ligands to the Zinc. Mutations in three of the four direct zinc ligands, C28, C209, and H234, showed severely deleterious defects on k_{cat} and K_m for cysteine in cysteinyl adenylate synthesis (Table 1). For example, the mutants C209S, H234S, and C28S/C209S had no measurable activity, while C28S was decreased in k_{cat}/K_m by 10^5-fold. In contrast, mutation of the E238 ligand had little effect. The apparently less important role of E238 in adenylate synthesis is consistent with structural studies showing that the E238−zinc distance lengthens significantly when sub-

Table 1: Kinetic Parameters of Adenylate Synthesis with Respect to Cysteine

	K_m (mM)	k_{cat} (s^{-1})	k_{cat}/K_m (s^{-1}M^{-1})	relative activity
wild type	0.031 ± 0.007	99.6 ± 7.8	3.23 x 10^6	1.0
C28S	2.36 ± 0.89	0.13 ± 0.04	5.59 x 10^1	1.73 × 10^{-5}
C209S	nd^a	nd		
H234S	nd	nd		
C28S/C209S	nd	nd		
E238S	0.05 ± 0.01	30.4 ± 1.2	6.08 × 10^5	1.9 × 10^{-1}
H234N/ E238Q	3.04	0.022	7.24	2.24 × 10^{-6}
C28S/ C209S/ H234N/ E238Q	nd	nd		
H206S	0.052 ± 0.013	37.8 ± 7.9	7.27 × 10^5	2.2 × 10^{-1}
H224S	2.78 ± 0.28	36.5 ± 0.48	1.31 × 10^4	4.06 × 10^{-3}
H235S	2.58 ± 0.59	1.32 ± 0.042	5.12 × 10^2	1.58 × 10^{-4}
H224S/ H235S	7.09 ± 0.49	8.98 ± 2.57	1.27 × 10^3	3.93 × 10^{-4}
H256S	0.21 ± 0.05	1.12 ± 0.04	5.33 × 10^3	1.65 × 10^{-3}
H234N/ E238Q/ H224N/ H235N	nd	nd		
W205F	2.52 ± 0.10	0.28 ± 0.02	1.09 × 10^2	3.39 × 10^{-5}
W205Y	3.61 ± 0.16	0.28 ± 0.01	7.64 × 10^1	2.36 × 10^{-5}
W205A	6.58 ± 4.22	0.22 ± 0.07	3.28 × 10^1	1.02 × 10^{-5}

^{a} Not detectable.

Table 2: Kinetic Parameters of Adenylate Synthesis with Respect to ATP

	K_m (mM)	k_{cat} (s^{-1})	k_{cat}/K_m (s^{-1}M^{-1})	relative activity
wild type	0.25 ± 0.002	141.9 ± 1.2	5.6 x 10^5	1.0
C28S	1.95 ± 0.94	0.35 ± 0.23	1.79 × 10^2	3.20 × 10^{-4}
C209S	nd	nd		
H234S	0.40	3.20 × 10^{-3}	8.01	1.42 × 10^{-5}
C28S/C209S	nd	nd		
E238S	0.98 ± 0.05	34.4 ± 0.6	3.5 × 10^4	6.2 × 10^{-2}
H234N/E238Q	1.70	0.0276	1.62 × 10^1	2.87 × 10^{-5}
C28S/C209S/ H234N/ E238Q	nd	nd		
H206S	0.37 ± 0.07	54.1 ± 12.5	1.46 × 10^5	2.6 × 10^{-1}
H224S	1.41	5.88 × 10^1	4.17 × 10^4	7.4 × 10^{-2}
H235S	1.57 ± 0.07	1.44 ± 0.01	9.17 × 10^2	1.62 × 10^{-3}
H224S/H235S	2.48 ± 1.08	31.1 ± 9.0	1.25 × 10^4	2.23 × 10^{-2}
H256S	0.42 ± 0.10	1.38 ± 0.48	3.28 × 10^3	5.8 × 10^{-3}
H234N/E238Q/ H224N/ H235N	nd	nd		
W205F	1.16 ± 0.21	0.55 ± 0.36	4.81 × 10^2	8.5 × 10^{-4}
W205Y	0.77 ± 0.22	0.29 ± 0.22	3.82 × 10^2	6.8 × 10^{-4}
W205A	0.69 ± 0.43	0.20 ± 0.10	2.96 × 10^2	5.2 × 10^{-4}

strate cysteine binds (Figure 1B). The double mutant H234N/E238Q, in which H234 and E238 were replaced by the structurally more similar asparagine and glutamine, respectively, was also severely defective. The quadruple mutant, in which all four ligands were substituted (C28S/C209S/H234N/E238Q), had no detectable activity.

Kinetic defects for ATP in adenylate synthesis were similarly deleterious (Table 2). Except for the E238S mutant, all mutants were substantially decreased in k_{cat}/K_m. For example, the C209S, C28S/C209S, and C28S/C209S/H234N/E238Q mutants each showed no measurable activity, while the H234S and H234N/E238Q enzymes were decreased by

Table 3: Kinetic Parameters of Aminoacylation with Respect to tRNA^{Cys}

	K_m (μM)	k_{cat} (s^{-1})	k_{cat}/K_m (s^{-1}M^{-1})	relative activity	Zn^{2+}/mol	K_d of tRNA^{Cys}
wild type	1.16 ± 0.01	2.46 ± 0.06	2.12×10^6	1.0	0.98 ± 0.07	0.32 ± 0.07
C28S	22.1 ± 10.5	5.63×0^{-3}	2.55×10^2	1.2×10^{-4}	0.78 ± 0.09	
C209S	63.5	4.13×10^{-3}	6.50×10^1	3.06×10^{-5}	1.10 ± 0.03	
C28S/C209S	95.2	5.27×10^{-3}	5.54×10^1	2.61×10^{-5}	0.66 ± 0.005	0.26 ± 0.08
H234S	57.6	1.8×10^{-2}	3.11×10^2	1.47×10^{-4}	1.05 ± 0.01	
E238S	0.83 ± 0.001	0.59 ± 0.06	7.1×10^5	3.3×10^{-1}		
H234N/E238Q	239.7 ± 153.6	0.03 ± 0.015	1.25×10^2	5.9×10^{-5}	0.84 ± 0.08	
C28S/C209S/H234N/E238Q	nd	nd			0.001 ± 0.009	
H206S	0.78 ± 0.32	1.08 ± 0.09	1.38×10^6	6.5×10^{-1}	1.04 ± 0.16	
H224S	2.14 ± 2.34	0.257 ± 0.066	1.20×10^5	5.7×10^{-2}	1.01 ± 0.13	
H235S	4.83 ± 2.34	0.039 ± 0.02	8.07×10^3	3.8×10^{-3}	0.98 ± 0.16	
H224S/H235N	23.2 ± 3.8	0.021 ± 0.001	9.0×10^2	4.24×10^{-4}	0.12 ± 0.01	
H256S	2.67 ± 0.21	0.57 ± 0.10	2.13×10^5	1.0×10^{-1}	1.07 ± 0.12	
H234N/E238Q/H224N/H235N	nd	nd			0.17 ± 0.004	0.23 ± 0.06
W205F			1.17×10^4	5.5×10^{-3}		
W205Y	6.62 ± 1.51	6.74×10^{-3}	1.02×10^3	4.8×10^{-4}		0.21 ± 0.04
W205A	4.89 ± 2.67	0.039 ± 0.018	0.8×10^4	3.77×10^{-3}		

10^3-10^4-fold. For these mutants, k_{cat} and, more significantly, K_m effects with respect to ATP were approximately 10-fold smaller than with respect to cysteine.

Kinetic parameters for tRNA^{Cys} in aminoacylation showed the same pattern (Table 3). The E238S mutant had the smallest defect (3-fold in k_{cat}/K_m), whereas all others were significantly diminished in activity (by 10^4-10^5-fold). For all mutants, the major defect was at the level of k_{cat}. Interestingly, decreases in tRNA aminoacylation were smaller than those observed in adenylate synthesis. Even mutants C209S, H234S, and C28S/C209S, which were completely inactive for adenylate synthesis, were weakly active for tRNA aminoacylation. The only mutant that was inactive for tRNA aminoacylation was the quadruple mutant that replaced all of the zinc ligands.

Mutations of the Histidine Array at the Base of the Active Site. Of the five histidines (H206, H224, H234, H235, and H256) at the base of the active site, substitution of the direct zinc ligand H234 had the largest effect on activity. This was followed in order by substitution of H235, H224 ∼ H256, and H206. For example, with respect to cysteine in adenylate synthesis (Table 1), the H234S mutant had no measurable activity, whereas the H235S mutant displayed a weak but measurable activity that was diminished by 10^4-fold from the wild type. The H224S and H256 mutants were each diminished by 10^2-fold, and the H206S mutant was diminished by less than 10-fold. This order of effect is preserved with respect to ATP in adenylate synthesis (Table 2), except that the effect of mutation is generally smaller. A double mutant, H224N/H235N, which altered two histidines in the array with the structurally similar asparagine, was as defective as the single H235S mutant. An additional substitution of two zinc ligands, H234N/E238Q, to this mutant generated a quadruple mutant that was inactive with respect to both cysteine and ATP (Tables 1 and 2).

Mutations in the histidine array also decreased tRNA aminoacylation (Table 3). The severity of catalytic reductions by substitutions was of the same order as that of adenylate synthesis (H234 > H235 > H224 ∼ H256 > H206), although the reductions were generally smaller. An exception was the double mutant H224N/H235N, which was reduced in adenylate synthesis with respect to cysteine by 10^3-fold and with respect to ATP by 10-fold (Tables 1 and 2), but

was reduced in aminoacylation by 10^3-fold (Table 3). Again, the quadruple mutant that derived from the double mutant had no aminoacylation activity.

Mutations of W205. The indole of the conserved W205 rotates into the amino acid pocket upon cysteine binding to stabilize the bound substrate (*14*). To test the role of this side chain, mutants W205A, W205F, and W205Y were analyzed. All three mutants showed a similar defect of 10^4-10^5-fold with respect to cysteine in adenylate synthesis (Table 1), a defect of 10^3-10^4-fold with respect to ATP (Table 2), and a defect of 10^2-10^3-fold in tRNA aminoacylation (Table 3). These were quantitatively similar to the corresponding reductions upon substitutions of the direct zinc ligands. For the three W205 mutants, the catalytic defects with respect to the three substrates, cysteine, ATP, and tRNA^{Cys}, were largely derived from the k_{cat} factor.

Because of the importance of W205 in stabilizing substrate in the cysteine-bound crystal structure, it was of interest to determine whether substitutions of this amino acid might relax substrate specificity. To test this possibility, activation of serine was measured in the presence of 0.5 M serine, 5 mM ATP, and 10 μM enzyme by the PP$_i$–ATP exchange assay. While the wild-type enzyme had no detectable activity (rate $< 10^{-3}$ s^{-1} M^{-1}), the W205Y mutant showed a weak activity with a rate of 0.03 s^{-1} M^{-1}. Other mutants, including W205F, W205A, C28S, C209S, C28S/C209S, H234S, H234S/E238Q, H224S, and H224N/H235N, were unable to activate serine. However, despite the 30-fold improvement in activation of serine over the wild type, the W205Y mutant showed no detectable activity in tRNA aminoacylation.

Zn^{2+} Content. Many mutants were analyzed for their Zn^{2+} content by atomic absorption spectroscopy (Table 3). Unexpectedly, most mutants retained high levels of zinc occupancy, even with substitutions of zinc ligands. For example, C28S, C209S, H234S, H234N/E238Q, and C28S/C209S, all of which contain substitutions of direct ligands that reduce activities to extremely low levels, still carried between 0.6 and 1.0 equiv of Zn^{2+}. Only removal of all four direct zinc ligands in the C28S/C209S/H234N/E238Q mutant caused loss of zinc binding. The H224N/H235N and H224N/H235N/H234N/E238Q mutants also bound very little zinc. The activities of each of these three enzymes were highly attenuated.
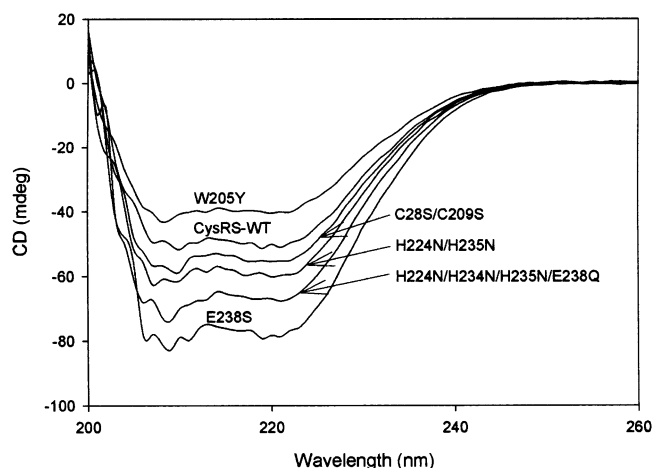
FIGURE 2: Circular dichroism spectra of the wild type and mutants of *E. coli* CysRS.
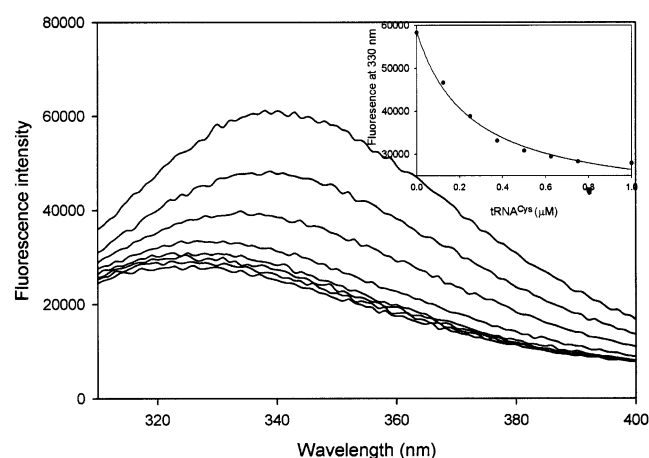

FIGURE 3: Fluorescence emission spectra of an equilibrium titration of *E. coli* CysRS with tRNA^{Cys}. The wild-type enzyme (0.625 μM) was incubated with tRNA^{Cys} over a range of 0.025−1.05 μM to derive a K_d of 0.32 μM (inset). Three mutants were analyzed similarly, which were C28S/C209S, W205Y, and H224N/H234N/H235N/E238Q.

Structural Integrity of Mutants. To test whether mutations in the CysRS amino acid cleft might perturb the enzyme structure, the structural integrity was probed by both circular dichroism (CD) and tRNA^{Cys}-binding affinity. The mutants tested were the active E238S, two mutants with weakened activity but high Zn^{2+}-binding capacity (C28S/C209S and W205Y), and two similarly weak mutants with low Zn^{2+}-binding capacity (H224N/H235N and H224N/H234N/H235N/E238Q). The CD spectra of the wild type were typical of a highly α-helical protein (Figure 2), and all five mutants exhibited similar spectra, verifying that secondary structure is retained.

Class I tRNA synthetases bind tRNA via global structural determinants (*20*, *21*), suggesting that tRNA^{Cys} binding by CysRS provides a reasonable probe of tertiary structural integrity. To quantitatively measure the affinity for tRNA^{Cys}, an equilibrium titration was developed on the basis of intrinsic tryptophan fluorescence (Figure 3). In this equilibrium assay, formation of the enzyme−tRNA complex was observed as a decrease of the fluorescence intensity. The excitation wavelength was chosen at 285 nm so as to obtain the highest emission spectrum. The emission wavelength was chosen at 330 nm such that the quench was specific to the

enzyme but not to the control tryptophan solution. BSA was not used as the control because there was no direct interaction with tRNA and no quench by the tRNA solution. Titration of 0.625 μM enzyme with increasing concentrations of tRNA yielded a series of fluorescence spectra, where the quench at 330 nm of each was monitored and corrected for the dilution factor. Analysis of fluorescence yields revealed a K_d of 0.32 μM for the wild type (Figure 3, inset), which was 3-fold smaller than the K_m of tRNA^{Cys} (1.16 μM) in the aminoacylation reaction (Table 3). This K_d is similar to those reported for tRNA binding by GlnRS and AspRS (*22*, *23*). By the same fluorescence titration, the K_d values of three of the five mutants mentioned above (C28S/C09S, W205Y, and H224N/H234N/H235N/E238Q) were determined and shown to be similar to that of the wild type (0.26, 0.21, and 0.23 μM, respectively). Interestingly, for the C28S/C209S and W205Y mutants, the K_d of tRNA binding was significantly smaller than the K_m of tRNA aminoacylation (Table 3). This suggests that while the overall enzyme affinity for the tRNA substrate did not change, the rate leading to formation of a catalytically productive enzyme−tRNA complex is likely reduced from that of the wild-type enzyme. The similarity in K_d values between the wild type and mutants was separately confirmed by a gel shift assay, where formation of the synthetase−tRNA complex was directly visualized and measured (data not shown).

DISCUSSION

A Well-Differentiated Zinc Center. Zinc is one of the most abundant and important first-row transition metals in enzymes. This metal ion can serve a purely structural role, such as in the zinc-finger motif of transcription factors, or it can serve a catalytic role, such as in the zinc enzymes carbonic anhydrase and carboxypeptidase A (*24*). In the catalytic role, the coordination geometries of the zinc change as the chemistry of catalysis proceeds. In CysRS, the zinc is at the active site, and its coordination geometry increases from four to five upon substrate binding (*14*, *15*). However, this does not directly assign a catalytic or structural role, because it has not been possible to isolate the zinc-free CysRS. Specifically, attempts to remove the zinc by using the strong metal chelator CDTA (*trans*-1,2-diaminocyclohexane-*N*,*N*,-*N′*,*N′*-tetraacetic acid) in the presence of 8 M urea, followed by dialysis in refolding buffer, resulted in precipitation of the enzyme. The inability to isolate the zinc-free enzyme prevented direct examination of the role of zinc in catalysis. To gain insights into the role of zinc, the direct zinc ligands and surrounding network of conserved side chains were mutated, and the purified mutants were characterized for enzyme activity and structural integrity. While the majority of substitutions lead to severe reductions of activity, many nonetheless retain the capacity to bind zinc. Of the few that lose the zinc (particularly the mutant H224N/H234N/H235N/E238Q), global structural integrity is maintained on the basis of the criteria of CD spectroscopy and tRNA binding. In addition, all mutants are well expressed in *E. coli* at levels over 70% of total cellular proteins, and all are stable in prolonged storage, suggesting preservation of the native structure regardless of the zinc-binding capacity. Together, these results suggest that zinc does not play a major role in the structural stability of the enzyme but, instead, a catalytic

function that is modulated by conserved side chains that surround the metal site.

Mutations to the conserved side chains have clear kinetic defects. First, although mutations affect both K_m and k_{cat} of all three substrates (cysteine, ATP, and tRNA^{Cys}), they generally have a stronger effect on k_{cat} than on K_m. This provides support for the notion that the amino acids in the zinc site help to build a substrate-binding site that precisely aligns the reactive α-carboxylate of the amino acid with respect to ATP and tRNA. Second, mutations tend to have a stronger effect on cysteine than on ATP in adenylate synthesis, which is consistent with the closer proximity of these side chains to the cysteine-binding cleft where the zinc is located. While most mutations are deleterious, E238S and H206S are relatively active. As noted in the crystal structures of *E. coli* CysRS, the E238−Zn^{2+} distance lengthens upon substrate binding, while H206S is at the periphery of the histidine array. In fact, the catalytic contributions of individual histidines in the array (as assessed by activities of the respective single mutants) are correlated with proximity to the zinc ion. The most important H234 directly ligates the zinc, while H235 lies 4.4 Å distant, and the least important H206 is separated by 6.9 Å.

Another general trend is that mutations have stronger effects on adenylate synthesis than on tRNA aminoacylation. This suggests that tRNA binding can partially repair local perturbations in the active site structure due to mutations. The possibility that tRNA binding might improve the efficiency of adenylate synthesis in the overall reaction may be general to tRNA synthetases. In fact, four class I synthetases, ArgRS, GlnRS, GluRS, and LysRS, must bind their cognate tRNA before catalysis of adenylate synthesis (*1*). The role of the tRNA in these cases is to rearrange the active site to properly align functional groups of the amino acid and ATP substrates for catalysis (*25*, *26*). The ability of tRNA to assist adenylate synthesis may be even applicable to those synthetases that catalyze adenylate synthesis in the absence of tRNA. For example, GlyRS, LysRS, and ThrRS have smaller K_m values for ATP in tRNA aminoacylation than in adenylate synthesis (*27*−*29*), suggesting that tRNA binding helps to structure the ATP-binding site. Also, tRNA binding in AspRS places the CCA end on top of the ATP site and helps to close the amino acid binding pocket (*30*). In the case of CysRS, the improved tRNA aminoacylation activity in mutants that are severely decreased for adenylate synthesis provides further support for the notion that the mutations have only local effects on structure.

The catalytic function of the zinc may be further enhanced by individual histidines at the base of the active site. Upon cysteine binding, the sulfhydryl proton of the cysteine thiol must be removed to form the enzyme-bound Zn^{2+}−thiolate. In solution the pK_a of the cysteine thiol is approximately 8.5; thus, some decrease in this value generated by the active site milieu appears likely to promote efficient catalysis at neutral pH. As in many zinc-catalyzed reactions, the histidine imidazole likely plays a role in modulating the electrostatic environments of the zinc center (*24*). In the crystal structures of *E. coli* CysRS, individual imidazoles in the histidine array are in or near H-bonding contact with each other, and all are located within 7 Å of the observed zinc site. Thus, these imidazoles can form a network of interactions that may orient and adjust the polarity of the zinc ligands, fine-tune the pK_a

and reactivities of theses ligands, and enhance the electrostatic interaction between the metal and the thiol of the substrate cysteine (*14*). The ability of these imidazoles to module the chemical properties of the zinc thus provides a shell of "indirect ligands" that can stabilize the catalytic transition state. The use of a shell of indirect ligands to modulate the activity of zinc is a common catalytic strategy employed by carbonic anhydrase and protein farnesyltransferase (*31*, *32*).

A Putative Second Zinc Site. An unexpected finding is that mutations of the direct zinc ligands do not result in a significantly decreased capacity for zinc binding. This is in contrast to the case of the structural zinc in *E. coli* MetRS, where a single mutation of the direct zinc ligand C148 significantly reduces the zinc occupancy (*33*, *34*). In CysRS, the retention of zinc-binding capacity, despite extensive mutations of directly ligating or nearby side chains, raises the possibility of a novel mechanism for its sequestration. Analysis of crystal structures of *E. coli* CysRS has suggested that several of the histidines in the array might cooperate to form a second zinc-binding site that consists of H224, H234, H235, C28, and E238 (*14*). Modeling suggests that a largely unencumbered movement of the zinc by about 2.5 Å from the first site, to the alternative position located deeper in the cysteine-binding cleft, can create the pentacoordination geometry of the second site. The putative second site may serve to allow shuttling of the zinc between the two sites. Although no precedent is known for a metal shuttle of this type, it is nonetheless conceivable that such a mechanism can offer substantial catalytic advantages. For example, movement of the zinc ion into the more distal second site after cysteinylation could allow one of the second site ligands (possibly H235) to more strongly bind the zinc and disrupt the Zn^{2+}−thiolate interaction at the first site, thus facilitating product release while retaining the metal on the enzyme for the next catalytic cycle. This is particularly important given that the intracellular concentration of free zinc in *E. coli* is extremely low (approximately femtomolar) (*35*), as most of the metal is tightly bound by the primary zinc sensor/regulator proteins. Alternatively, the second zinc site may help to facilitate structural rearrangement leading to rejection of noncognate amino acids. Because three of the amino acids proposed in the second site are shared in common with those of the first site, the two sites should be mutually exclusive in binding the zinc, which explains the identification of only one zinc in the existing crystal structures as well as the atomic absorption measurements indicating the presence of one zinc ion per protein chain. Structure determinations of mutant enzymes, perhaps containing the C209S mutation within the observed zinc site, or of enzyme complexes with tRNA at later stages of the catalytic cycle may allow observation of a zinc ion trapped in the proposed second site.

The existence of a second zinc site is also suggested by the difficulty in removing zinc from wild-type CysRS. As mentioned above, even the combination of CDTA and 8 M urea does not effectively remove the zinc (*15*). Possibly, disruption of the zinc site by partial denaturation may allow the metal to reside in the second site. Additional evidence for the second site is provided by atomic absorption analysis of CysRS mutants (Table 3). The observed zinc site is resistant to mutation: all single mutants and even the C28S/

C209S and H234N/E238Q double mutants retain high levels of zinc, suggesting the possibility that in these enzymes the zinc may be bound in the intact second site. Similarly, the H234N/E238Q double mutant in the observed zinc site binds zinc well, but addition of the H224N and H235N substitutions in the proposed second site produces a quadruple mutant that no longer retains the metal. More strikingly, the double mutant H224N/H235N, which contains no mutation in the first zinc site but has removed two of the putative contacts in the second site, is greatly decreased in zinc content. It appears that if the second site exists, its integrity is important as mutations at this site can prevent the zinc ion from binding to the first site. Certainly, additional studies to test the possibility of a second zinc site are necessary. Regardless of whether the zinc shuttling mechanism in fact is proved, we wish to emphasize that the existence of five strictly conserved histidines adjacent to the active site, with a unique configuration unprecedented in protein structural databases, very strongly implies a specific catalytic role beyond simply serving to lower the pK_a of the active site cysteines for zinc binding.

Implications for Enzyme Specificity. The well-differentiated zinc center of CysRS is conserved in all three major domains of life (*14*), indicating a strong evolutionary pressure that selectively developed this structure. The inherently strong and favorable zinc−thiolate interaction allows discrimination against serine without the need for an editing step. In contrast, the class II ThrRS, which is the only other synthetase that relies on zinc for amino acid selection, uses the metal to coordinate with the hydroxyl group of the substrate threonine (*9, 10*). By forming the less favorable zinc−oxygen interaction in its inner sphere, ThrRS cannot sufficiently discriminate against serine and requires a separate editing step to hydrolyze misactivated serine.

The elaborate structure of the zinc center in CysRS suggests that attempts to engineer alternative amino acid specificities into the enzyme will not be easy and will perhaps require large-scale alterations of the amino acid binding pocket. Indeed, only the W205Y mutant among those examined is able to weakly activate serine. The ability of the W205 mutant to activate serine is not due to improved binding of serine, as has been verified by spectroscopic studies (*15*). Rather, it must derive from rearrangement of the active site that may promote improved alignment of catalytic groups. Nonetheless, activation of serine by the W205Y mutant is at least 30-fold higher than by the wild-type enzyme, decreasing the discrimination factor against serine from perhaps 10^8-fold to 10^6-fold (*13, 15*). This does not seriously threaten the accuracy of protein synthesis, as the overall error rate in vivo is about 1 in 3000 (*36*). Moreover, the W205Y mutant does not transfer serine to tRNA^{Cys}. This suggests an additional discrimination against serine provided by the larger tRNA substrate, which may be evolutionarily significant during development of specificity and which further reveals an important interplay between the tRNA and amino acid binding sites.

REFERENCES

1. Schimmel, P. R., and Soll, D. (1979) *Annu. Rev. Biochem. 48*, 601−648.

2. Cusack, S. (1997) *Curr. Opin. Struct. Biol. 7*, 881−889.

3. Ibba, M., and Soll, D. (2000) *Annu. Rev. Biochem. 69*, 617−650.

4. Freist, W. (1989) *Biochemistry 28*, 6787−6795.

5. Schmidt, E., and Schimmel, P. (1994) *Science 264*, 265−267.

6. Nureki, O., Vassylyev, D. G., Tateno, M., Shimada, A., Nakama, T., Fukai, S., Konno, M., Hendrickson, T. L., Schimmel, P., and Yokoyama, S. (1998) *Science 280*, 578−582.

7. Fukai, S., Nureki, O., Sekine, S., Shimada, A., Tao, J., Vassylyev, D. G., and Yokoyama, S. (2000) *Cell 103*, 793−803.

8. Cusack, S., Yaremchuk, A., and Tukalo, M. (2000) *EMBO J. 19*, 2351−2361.

9. Sankaranarayanan, R., Dock-Bregeon, A. C., Romby, P., Caillet, J., Springer, M., Rees, B., Ehresmann, C., Ehresmann, B., and Moras, D. (1999) *Cell 97*, 371−381.

10. Sankaranarayanan, R., Dock-Bregeon, A. C., Rees, B., Bovee, M., Caillet, J., Romby, P., Francklyn, C. S., and Moras, D. (2000) *Nat. Struct. Biol. 7*, 461−465.

11. Beuning, P. J., and Musier-Forsyth, K. (2000) *Proc. Natl. Acad. Sci. U.S.A. 97*, 8916−8920.

12. Schreier, A. A., and Schimmel, P. R. (1972) *Biochemistry 11*, 1582−1589.

13. Fersht, A. R., and Dingwall, C. (1979) *Biochemistry 18*, 1245−1249.

14. Newberry, K. J., Hou, Y. M., and Perona, J. J. (2002) *EMBO J. 21*, 2778−2787.

15. Zhang, C. M., Christian, T., Newberry, K. J., Perona, J. J., and Hou, Y. M. (2003) *J. Mol. Biol. 327*, 911−917.

16. Maret, W., and Vallee, B. L. (1993) *Methods Enzymol. 226*, 52−71.

17. Fersht, A. R., Ashford, J. S., Bruton, C. J., Jakes, R., Koch, G. L., and Hartley, B. S. (1975) *Biochemistry 14*, 1−4.

18. Cole, F. X., and Schimmel, P. R. (1970) *Biochemistry 9*, 480−489.

19. Hou, Y. M., Westhof, E., and Giege, R. (1993) *Proc. Natl. Acad. Sci. U.S.A. 90*, 6776−6780.

20. Delagoutte, B., Moras, D., and Cavarelli, J. (2000) *EMBO J. 19*, 5599−5610.

21. Rould, M. A., Perona, J. J., Soll, D., and Steitz, T. A. (1989) *Science 246*, 1135−1142.

22. Bullock, T. L., Sherlin, L. D., and Perona, J. J. (2000) *Nat. Struct. Biol. 7*, 497−504.

23. Frugier, M., Moulinier, L., and Giege, R. (2000) *EMBO J. 19*, 2371−2380.

24. Christianson, D. W. (1991) *Adv. Protein Chem. 42*, 281−355.

25. Francklyn, C., Perona, J. J., Puetz, J., and Hou, Y. M. (2002) *RNA 8*, 1363−1372.

26. Sherlin, L. D., and Perona, J. J. (2003) *Structure 11*, 591−603.

27. Freist, W., Logan, D. T., and Gauss, D. H. (1996) *Biol. Chem. Hoppe-Seyler 377*, 343−356.

28. Freist, W., and Gauss, D. H. (1995) *Biol. Chem. Hoppe-Seyler 376*, 451−472.

29. Freist, W., and Gauss, D. H. (1995) *Biol. Chem. Hoppe-Seyler 376*, 213−224.

30. Cavarelli, J., Eriani, G., Rees, B., Ruff, M., Boeglin, M., Mitschler, A., Martin, F., Gangloff, J., Thierry, J. C., and Moras, D. (1994) *EMBO J. 13*, 327−337.

31. Hunt, J. A., Ahmed, M., and Fierke, C. A. (1999) *Biochemistry 38*, 9054−9062.

32. Harris, C. M., Derdowski, A. M., and Poulter, C. D. (2002) *Biochemistry 41*, 10554−10562.

33. Mechulam, Y., Schmitt, E., Maveyraud, L., Zelwer, C., Nureki, O., Yokoyama, S., Konno, M., and Blanquet, S. (1999) *J. Mol. Biol. 294*, 1287−1297.

34. Landro, J. A., and Schimmel, P. (1993) *Proc. Natl. Acad. Sci. U.S.A. 90*, 2261−2265.

35. Outten, C. E., and O'Halloran, T. V. (2001) *Science 292*, 2488−2492.

36. Loftfield, R. B., and Vanderjagt, D. (1972) *Biochem. J. 128*, 1353−1356.